land

MDPI

Article

Analysis of landslide Susceptibility and Tree Felling Due to an Extreme Event at Mid-Latitudes: Case Study of Storm Vaia, Italy

Guido Antonetti, Matteo Gentilucci *, Domenico Aringoli and Gilberto Pambianchi

School of Science and Technologies, Geology Division, University of Camerino, 62032 Camerino, Italy
* Correspondence: matteo.gentilucci@unicam.it

Abstract: Storm Vaia on 29 October 2018, hit northeastern Italy and produced extensive damage in the immediacy of the event, including extensive tree felling in some places, as well as debris flow or earth flow landslides. This study aims to assess the susceptibility of the area following extreme events by evaluating the environmental criticality during strong winds and intense precipitation. Specifically, tree felling susceptibility due to wind and landslide susceptibility due mainly to precipitation were analysed by taking into consideration the geomorphological and environmental criticality of the areas under study. In particular, the area was modelled using fluid dynamics software, allowing an understanding of wind accelerations in relation to morphology, showing excellent agreement between the tree falls that occurred during the event and the areas with the highest wind gusts. With regard to landslides, an algorithm was prepared through GIS software that took into account the debris and earth flows that were activated during the extreme event in question, allowing the creation of a susceptibility map that delineated areas of high potential hazard. The final result is a landslide and tree-fall susceptibility map that determines the fragility of the territory during an extreme event. The procedures applied in the study area can be considered as a working method that allows critical values to be obtained for extreme events that can produce damage to the environment and beyond. It follows that this research also has an immediate application purpose by helping the political decision-maker in the choice of interventions to be implemented.

Keywords: wind gust; wind; extreme event; storm; susceptibility; landslides; debris flow; GIS

Citation: Antonetti, G.; Gentilucci, M.; Aringoli, D.; Pambianchi, G. Analysis of landslide Susceptibility and Tree Felling Due to an Extreme Event at Mid-Latitudes: Case Study of Storm Vaia, Italy. *Land* **2022**, *11*, 1808. https://doi.org/10.3390/land11101808

Academic Editor: Nir Krakauer

Received: 17 September 2022
Accepted: 12 October 2022
Published: 15 October 2022

1. Introduction

Extreme events are becoming increasingly frequent around the world, and increasingly energetic, with often catastrophic results [1,2]. Global warming favours this process, as the emission of greenhouse gases increases the energy within the atmosphere, thus producing atmospheric phenomena characterised by greater energy than a few decades ago [3]. Italy is no exception; in fact, it is at a crossroads in terms of atmospheric circulation, caught between polar and tropical air masses that alternate and give rise to intense weather phenomena [4]. These events alert territorial institutions, which are faced with massive economic damage to infrastructure and in the most severe cases human lives, so that it is important to increase territorial resilience to disasters. Extreme weather events produce many negative effects, especially in relation to slope stability, where rain has the effect of triggering quiescent landslides in many cases [5,6]. Other climatic parameters have different peculiarities than rain in the case of an extreme event; for example, wind can produce harm directly to buildings and infrastructure, so much so that in the most intense cases it can cause damage or extensive felling of plants [7]. Temperature and drought events are typically weather parameters that do not produce immediate effects like a thunderstorm, but are extreme events that are all the more damaging the longer they last. In the latter case, problems such as water supply [8] are exacerbated, there may be damage to the harvest for certain types of crops [9], and, if climate change is persistent, it could even lead to adaptation problems for plant species [10], as has already been observed in marine biology [11]. In this

case, those geological–geomorphological and environmental criticalities, originating in the immediacy of the event with a clear cause-and-effect relationship with the climatic variable that produced them, were studied. This led to the preparation of a landslide susceptibility map based on the landslides triggered during storm Vaia, and wind modelling was carried out to highlight the areas most susceptible to wind damage. Landslide susceptibility maps have been numerous in recent decades, with a wide variety of statistical methods and with more or less climatic–environmental parameters on which to calibrate the model. Among the most widely used and successful statistical methods are logistic regression [12], neural network analysis [13], data-overlay [14], index-based [15], and weight-of-evidence [16] methods, with an increasing trend toward analysis by machine learning methods in recent years [17]. As for the appropriate climatic–environmental data to provide a discriminant to the various areas analysed, they have not changed much since a few decades ago; slope gradient, exposure, land use, geological substrate, hydrographical network density, precipitation, etc. are very often taken into consideration [18,19]. Much rarer, on the other hand, are the susceptibility maps referred, as in the case of the present research, to an extreme event; in fact, although there are some examples, they are nevertheless mainly related to the study area that has generally already been the site of a disaster [20]. Regarding the susceptibility of vegetation to extreme events, particularly referring to forests, the most influential extreme event parameter was wind gust speed. In many cases, classifications of forest species subject to greater damage in relation to extreme wind events have been made, although most often they were made a priori without a real test of the wind or resilience of the plant species [21]. Some scientific research, on the other hand, tends to use algorithms to estimate the probability of wind damage depending on the ecosystem conditions of the study area, in terms of topography, soil type, etc. [22]. In other cases, the change in plant growth paths by intense wind events were examined [23]. Other fields of research vary in the factors of plants that tend to amplify wind damage [24], although the analysis of wind in relation to fire risk is much more common [25]. The purpose of this study is to assess the landslide susceptibility and the susceptibility of forest vegetation to felling in the case of an extreme event such as storm Vaia. Therefore, the aim is to assess two types of criticalities, one geomorphological, the other vegetational, trying to obtain a model that can provide an analysis of environmental susceptibility from extreme events, in order to identify the most vulnerable areas in these cases and improve spatial planning. Landslide susceptibility was treated through an algorithm that initially analysed the landslides that occurred during storm Vaia and then generalised the observations by extending them to the surrounding area. As for the felling of forest species due to high wind speeds, a model was used taking into account the gust speeds of some weather stations in the area, integrating the value over the territory and evaluating it in relation to the most damaged areas. The innovativeness of the research lies both in combining these two types of environmental vulnerability and in the methods used, in terms of event modelling. In particular, the results were very significant because the areas were differentiated in relation to the landslide hazard of the event, and great agreement was found between the areas subject to tree felling following the event and the higher wind gust values obtained using the model. This research proposes a methodology to better manage the territory following an extreme event, making it possible to foresee possible dangerous situations and resolve them with the appropriate naturalistic interventions.

2. Materials and Methods

2.1. Study Area

The Feltrino area is a geographic area located in the southwestern part of the province of Belluno, between the Dolomite zone and the pre-Alpine chain, in northeastern Italy. It is very well differentiated in terms of altitude, ranging from the lowest valley at 230 m a.s.l. to the highest peaks at 2229 m a.s.l. It is characterised by a so-called 'bowl' shape because the entire area is surrounded by mountains (Figure 1).

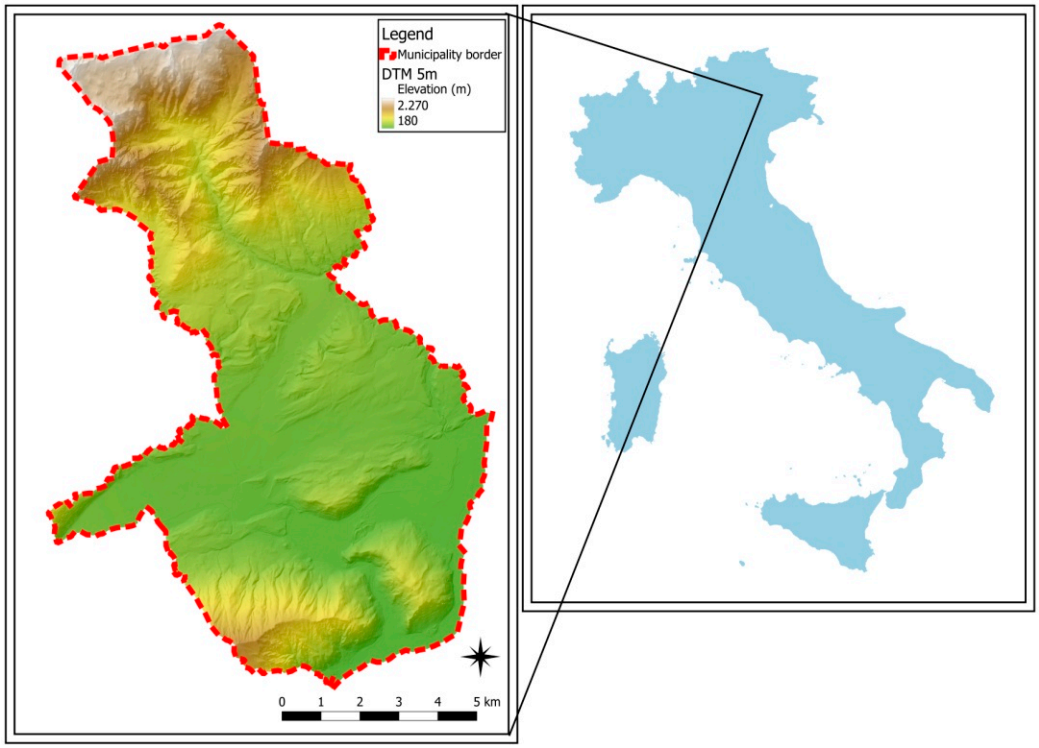

Figure 1. Geographic map of the municipality of Feltre.

The municipality of Feltre belongs to the Piave river basin, whose tributaries are some of the main watercourses flowing through the city, such as Caorame, Colmeda, Stien, Stizzon, and Sonna. The characteristic morphological elements of the territory are the wide Val Belluna, which almost coincides with the Belluno syncline, and the two other main valleys with a north–south direction, Val di San Martino and Val di Lamen. In the Quaternary period, the territory went through a complex evolution with the development of different landforms and the deposition of sedimentary sequences from different processes. These deposits are very well preserved in some places due to major gravitational phenomena that buried them, while in other areas they are completely obliterated. In the area there are a large number of landslides and gravitational deposits due to the very deep incisions of the hydrographic network and the poor mechanical quality of some rock types with layers of limestone and silt, Fonzaso Formation and Flysch Bellunese. Climatically, the Feltre area must be considered a temperate and humid continental climate zone like all areas on the southern side of the Alps. The average annual temperature over a 26-year series is 10.7 °C and the cumulative annual precipitation on the same data base is 1613 mm. These parameters classify the area as Dfd according to the Köppen–Geiger classification, a humid continental area with cold winters, because at least one month has an average temperature below −3 °C [26].

2.2. Storm Vaia

Vaia is the name given to the hurricane that hit all of northeastern Italy on 29 October 2018 (Figure 2).

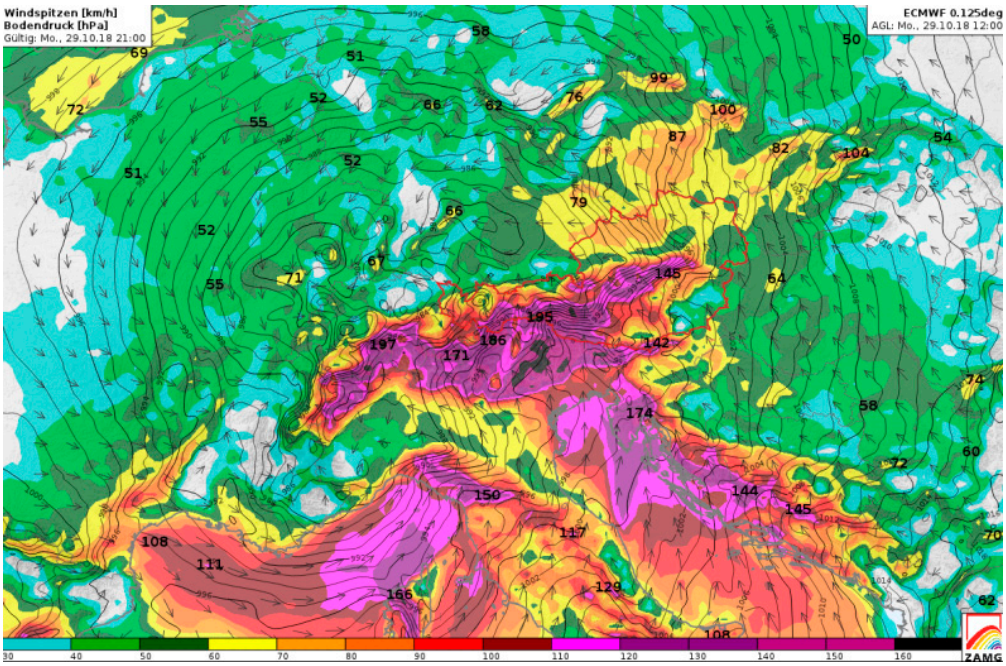

Figure 2. Synoptic chart for storm Vaia on 29 October 2018 (ECWMF, European Centre for Medium-Range Weather Forecasts).

This event is considered the worst climatic disaster to hit the Veneto region, worse even than the 1966 flood. This extreme event was generated by a perturbation that crossed the study area between 27 and 30 October 2018. A low-pressure centre stabilised in the Gulf of Genoa received moist air from the western and central Mediterranean, which increased the relative low pressure on the ground. On 27 October, it was characterised by persistent rainfall, with weak to moderate intensity, especially in mountainous areas with local snowflakes on the highest peaks. On the 28th of October, the disturbance evolved into more intense and widespread rainfall, which ceased in the evening, while a strong southerly wind blew in the pre-alpine region. There was no precipitation in the early hours of 29 October, but then a disturbance from the south began to intensify and produce persistent, heavy rain over the region. In the late morning hours, a strong Sirocco wind began to blow, reaching unusually high speeds, especially in the valleys and generally over the entire area, with peaks of 190/200 km/h. On 30 October, the already weakened rainfall began to cease.

2.3. Landslides Activated during the Event

During storm Vaia, nine landslide movements were triggered, and these were identified, photographed, and characterised [27]. They were then used to assess landslide susceptibility in the event of an extreme precipitation event of the same magnitude as storm Vaia.

- **Code 025021_01c**: Rotational slip with retrogressive evolution due to water concentration. Landslide in overconsolidated moraine materials (Figure 3).
- **Code 025021_02c**: Rotational slip due to water overpressure, with erosion and debris flow to the underlying road section. Face L = 10 m, H = 5 m, Sp = 2–3 m. These are well-graded sands and gravels of fluvio-glacial origin, very compact and fairly permeable (Figure 4).

Figure 3. Landslide photograph code 025021_01c.

Figure 4. Landslide photograph code 025021_02c.

- **Code 025021_03c**: Rotational sliding with retrogressive evolution due to water concentration of road water (Figure 5). Landslide in conglomeric and fluvioglacial materials. Face L = 10 m, H = 10 m, Sp = 1–2 m.

Figure 5. Landslide photograph code 025021_03c.

- **Code 025021_04c**: Landslide of loose cover downstream of the roadway due to oversaturation of soils rich in silty-clay matrix (Figure 6). The roadbed collapsed over a length of approximately 20 m. The gabion walls built in the past have shifted about 1 m downstream.

Figure 6. Landslide photograph code 025021_04c.

- **Code 025021_05c**: This landslide is characterised by two different movements at short distances: one (visible in Figure 7) a rotational sliding landslide, due to water concentration on fluvioglacial materials, with abundant silty–clay matrix and highly variable permeability, the other (Figure 8) a translational sliding landslide affecting a large arenaceous–siltitic mass.

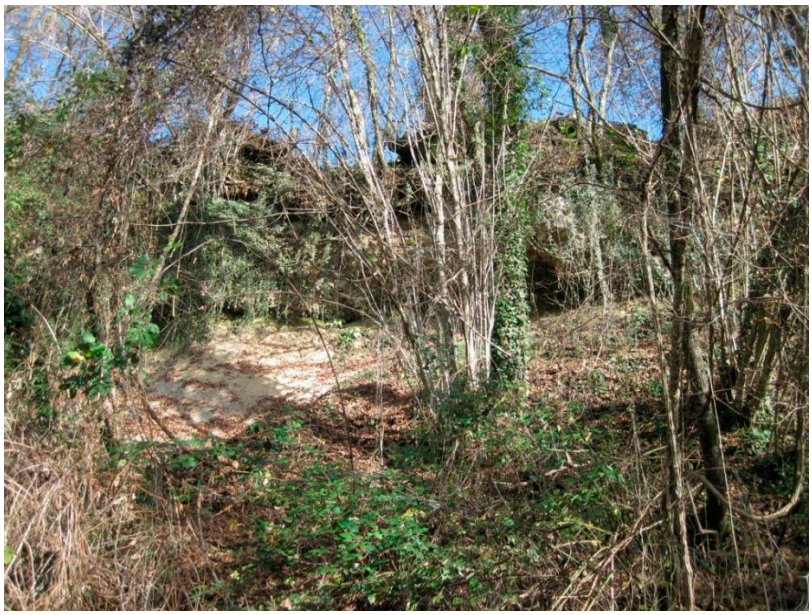

Figure 7. Landslide photograph code 025021_05c, rotational sliding.

Figure 8. Landslide photograph code 025021_05c, translational sliding.

- **Code 025021_06c**: Rotational slip at a moraine terrace, due to hypodermic water concentrations in the most permeable levels that saturated the material with a high silt–clay matrix (Figure 9). The moraine material is normally overconsolidated, with stable 35–40° slopes. Landslide face L = approx. 20 m, H = 4–5 m, thickness = 1–2 m.

Figure 9. Landslide photograph code 025021_06c.

- **Code 025021_07c**: Landslide of the roadside due to subsurface slope failure caused due to erosion of the river Sonna at the foot. Short slope in loose gravelly materials (Figure 10).

Figure 10. Landslide photograph code 025021_07c.

- **Code 025021_08c**: Sliding landslide of loose cover from water concentration during recent events (Figure 11).

Figure 11. Landslide photograph code 025021_08c.

2.4. Landslide Susceptibility Analysis Method

Landslide susceptibility analysis is a very topical issue; however, in this case, the susceptibility analysis is performed in relation to an extreme evet, so extremely precipitation-dependent phenomena such as debris or earth flows were taken into account [27]. From an operational point of view, no less than 9 landslides were identified immediately after the event and reactivated. These landslides were studied through 8 geological–geomorphological and vegetation parameters that characterised the landslide zone: permeability of the lithotype, type of vegetation cover, aspect, slope, type of substrate, deposits, recent deposits, and landslide map. The slope was divided into classes arbitrarily on the basis of other similar research, The aspect was differentiated by taking into account that the wind rose into 8 classes of 45° each. Permeability, on the other hand, was divided into very low, low to medium, medium to high, and very high, dividing it between porosity in deposits and fracturing in rocks. The vegetation was based on the subdivision of the area carried out by ISPRA (Istituto Superiore per la Protezione Ambientale, Higher Institute for Environmental Protection) in 2010 [28], while the geological characterisation and the deposits characterisation were based on the geological map sheet of Belluno [29].Finally, the presence of landslides and their activation status were analysed by means of the PAI (Piano di Assetto Idrogeologico, Hydrogeological Structure Plan, drawn up by the Basin Authority of the Isonzo, Tagliamento, Livenza, Piave, and Brenta-Bacchiglione rivers) This landslide susceptibility analysis was inspired by the weight of evidence [15]; however, it is a more conservative and precautionary method, because it does not discriminate parameters by assigning them a value, but rather only verifies the presence of a given parameter. The analysis was carried out using the QGIS software tool, which made it possible to assess the characteristics of each individual area on the basis of the chosen parameters that produce an increase in landslide susceptibility. A QGIS 'extraction by location' tool made it possible to extract all geological–geomorphological and vegetation features under each individual landslide triggered by storm Vaia. Subsequently, a series of 'clips' was made between polygons according to the level, so that each polygon was clipped with each of the others, and then 'merge' was performed to create the level.

2.5. Tree Felling Susceptibility Analysis Method

In order to analyse the study area in detail, a DEM digital elevation model with a grid resolution of 10 m was used (Figure 12) [30]. The evaluation of the felling that occurred during storm Vaia was performed using various types of methods. Primarily, a

general assessment of the areas of interest was performed by analysing the change in the Normalized Difference Vegetation Index (*NDVI*) value of the areas before and after the event. This satellite index makes it possible to assess the amount of foliage and therefore healthy vegetation, as it is proportional to the photosynthesis capacity of a plant.

$$NDVI = (NIR - RED)/(NIR + RED) \quad (1)$$

where NIR is near infrared radiation, between 780 and 1400 nm of wavelength, and RED is red radiation, between 650 and 780 nm of wavelength.

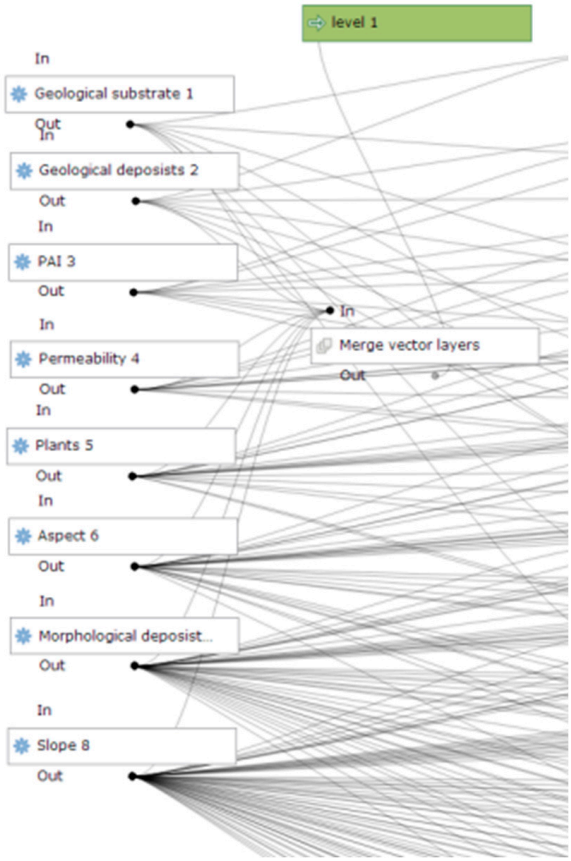

Figure 12. Architecture of the first level of susceptibility.

In this case, Sentinel-2 maps with a resolution of 10 m were used to calculate the NDVI and the image processing level used was L1C. Using QGIS software, these satellite images were processed and the NDVI was calculated based on the procedure described above; the acquisition took place once before the event on 11 October 2018 and once after the event on 31 October 2018, selecting days with negligible cloud cover. The value of the NDVI can vary between −1 and 1; a value of −1 is associated with bodies of water, while values between 0 and 0.2 are associated with bare soil. NDVI values between 0.2 and 0.4 correspond to areas with sparse vegetation; moderate vegetation tends to vary between 0.4 and 0.6; and anything above 0.6 indicates the highest possible density of green leaves [31]. The wind gust was then modelled with WindNinja software [32], software that applies fluid dynamics to spatialise the wind on a topographic surface. Data from 7 weather stations in the area with anemometers were entered into the model: Sospirolo, 426 mslm; Monte Avena, 1415 mslm; Lamon, 650 mslm; Feltre, 264 mslm; Quero, 252 mslm; and Santa Giustina Bellunese, 278 mslm (Figure 13).

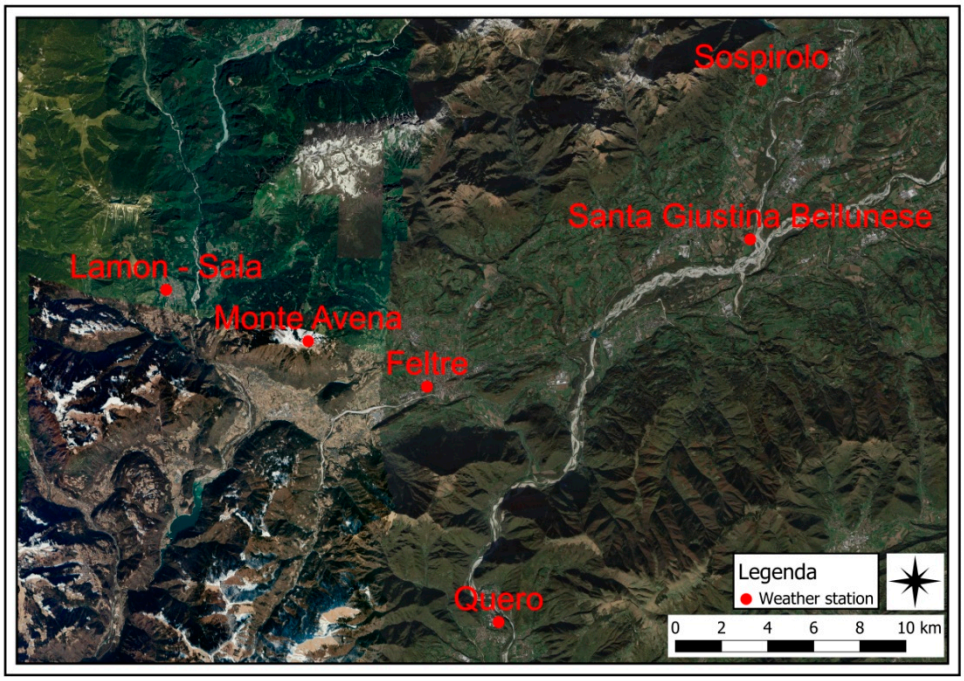

Figure 13. The 6 weather stations collected to calculate the wind gust model.

Data from these weather stations were collected by entering them into a Microsoft Excel 2007 file, in terms of prevailing wind direction, average wind speed, and gust speed, with hourly and daily temporal resolution. For the entire process, some of the analyses and the final cartographic product were carried out using QGis software.

3. Results

3.1. Landslide Susceptibility Analysis

The identification of nine landslides within the municipal territory of Feltre, which were triggered during storm Vaia, led to the analysis of the geomorphological–environmental conditions that characterised the landslide portions of the territory (Figure 14).

Six parameters were identified that influence slope stability in the case of an extreme precipitation event. The first result of this research was to assess whether all the landslides activated during the event had the eight chosen parameters coinciding; this was the starting point of the research, because it allowed the isolation of debris flow or earth flow landslide activation conditions. To simplify data extrapolation, each parameter was divided into classes (Table 1). Table 1 expresses, with the columns, the different classes used to differentiate the territory according to susceptibility to a landslide event during an extreme event; obviously, the more susceptible the territory is, the more features it has in common with the nine landslides triggered during storm Vaia (Figure 15).

Table 1. Geomorphological and environmental parameters divided into classes for the assessment of landslide susceptibility.

Slope	Aspect	Permeability	Vegetational Cover	Geological Formation	Deposits	Recent Deposits	Landslide Map
0–3°	338–22°	Very low	Salix	Vajont limestone	Thickened granular materials of ancient fluvial and/or fluvioglacial terraces with a predominantly gravelly and sandy texture	Alluvial and conoid deposits	Present
4–9°	23–67°	From low to medium	Quercus robur, Quercus petraea, and Carpinus betulus	Dolomia of St. Boldo	Heterogeneous-textured materials from torrential dejection cone deposits	Slopes and debris cones	Not present
10–18°	68–112°	From medium to high	Pinus sylvestris	Main Dolomia	Loose material from recent and current deposition of the mobile riverbed and recent flooding areas	Moraine deposits	
18–27°	113–157°	Very high	Picea abies	Igne formation	Coarse fluvioglacial or moraine accumulation materials in a fine sandy matrix		
27–45°	158–202°	Very low	Quercus petraea, Carpinus betulus	Formation of Soverzene	Colluvial and eluvial debris cover		
>45°	203–247°	From low to medium	Pinus mugo	Schiara Dolomia			
	248–292°	From medium to high	With high human influence	Ammonitic Red			
	293–337°	Very high	Fagus	Limestone of Campo-torondo			
			Castanea sativa and Quercus Petraea	Formation of Fonzaso			
			Shrubby areas	Biancone			
			Grassland and elevated plateau	Soccher limestone			
			Maple, ash, and linden	St. Vigilio Group			
				Grey limestones			
				N. Dolomia			
				Bellunese flysch			
				Red flake			
				Cinereous flake			
				Marl of the Golden Vein			
				Glauconitic sandstone of Belluno			
				S. Gregorio sandstone			
				Sandstone of M. Baldo			

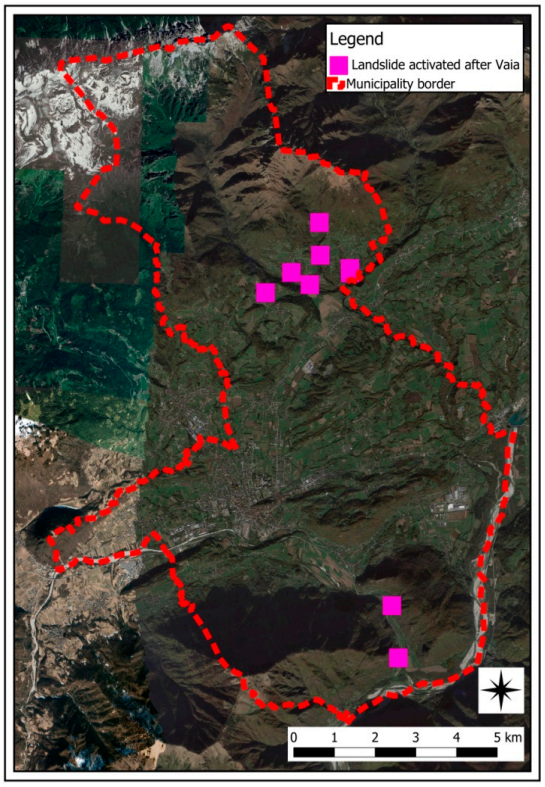

Figure 14. True-colour satellite image (Bands 4, 3, 2) from the Sentinel-2 satellite, showing the location of the 9 landslides triggered during storm Vaia, shown in fuchsia.

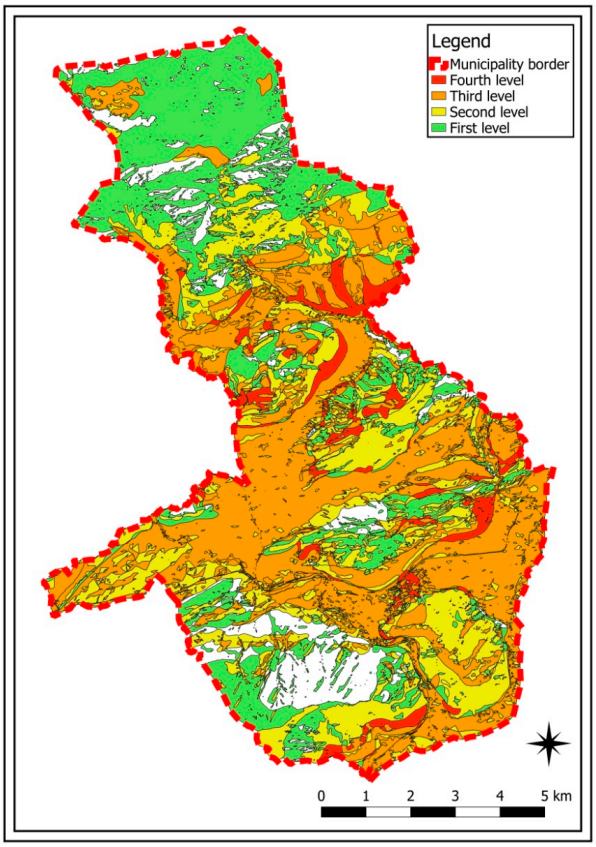

Figure 15. Susceptibility map for extreme precipitation events in the municipality of Feltre.

3.2. Analysis of the Susceptibility of Forest Species to Felling

In order to produce a susceptibility analysis of forest species from an extreme wind event, it is necessary to go through several steps. First, areas with a high number of windthrow trees caused by storm Vaia were mapped; the areas were identified using GIS software on the basis of the census conducted by the municipality of Feltre (Figure 16). In particular, the census conducted and subsequently digitised, in Figure 16, shows the different percentages of broken trees, uprooted trees, broken and uprooted trees, and undefined damage in the different areas.

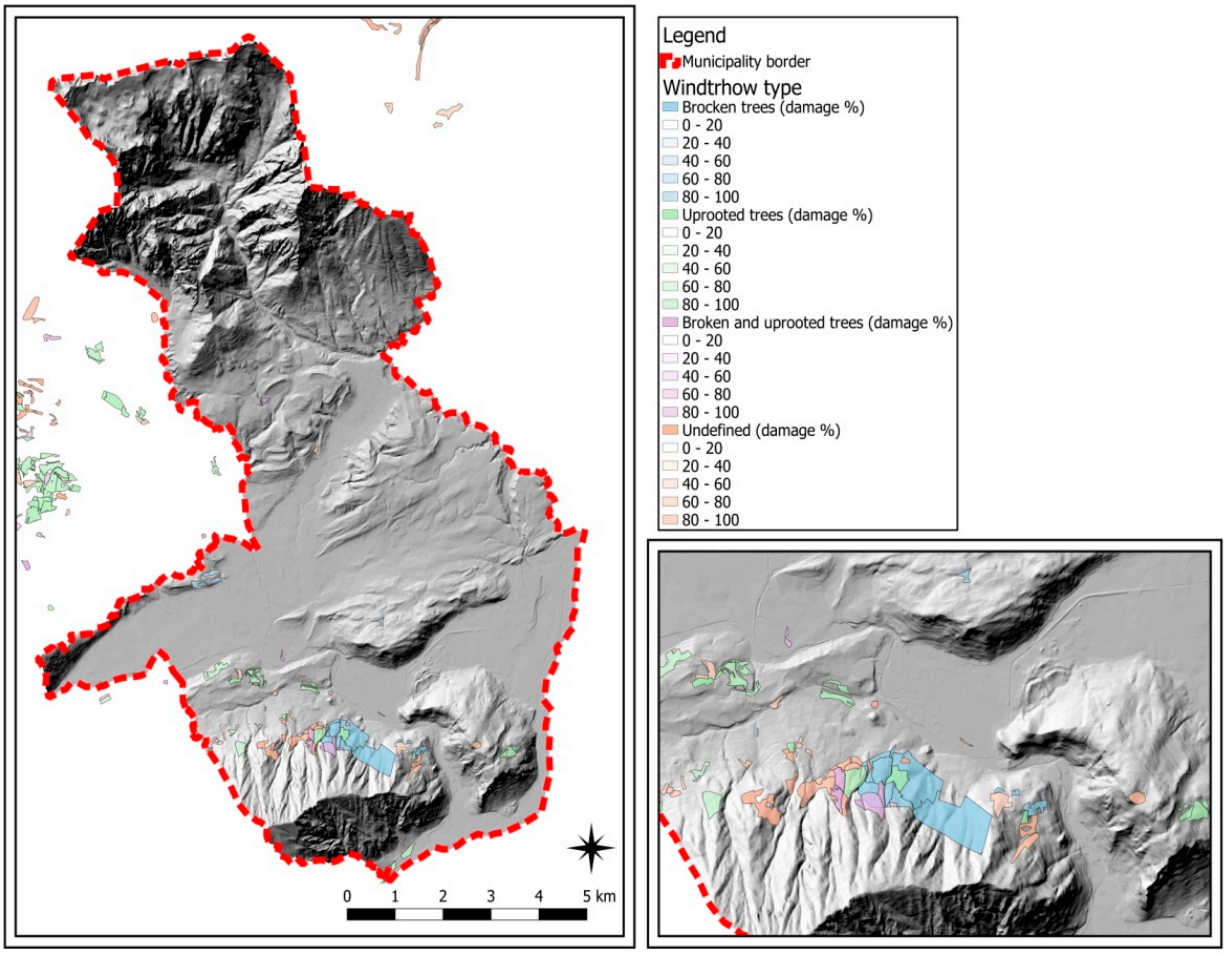

Figure 16. Map of windthrown types, which are differentiated into four categories: broken trees in blue, uprooted trees in green, broken and uprooted trees in purple, and undefined trees in brown. The increasing percentage of windthrown is represented for each category with the abovementioned brighter colours.

In parallel, the NDVI was calculated before and after the Vaia storm in order to assess the differences in live vegetation between the two satellite maps. Hence, satellite analysis using the NDVI confirmed the correctness of the census, highlighting areas with windfall trees (Figure 17). Figure 17 shows a general decrease in live vegetation throughout the Feltre municipality, with the greater presence of the colour red indicating predominantly bare soils.

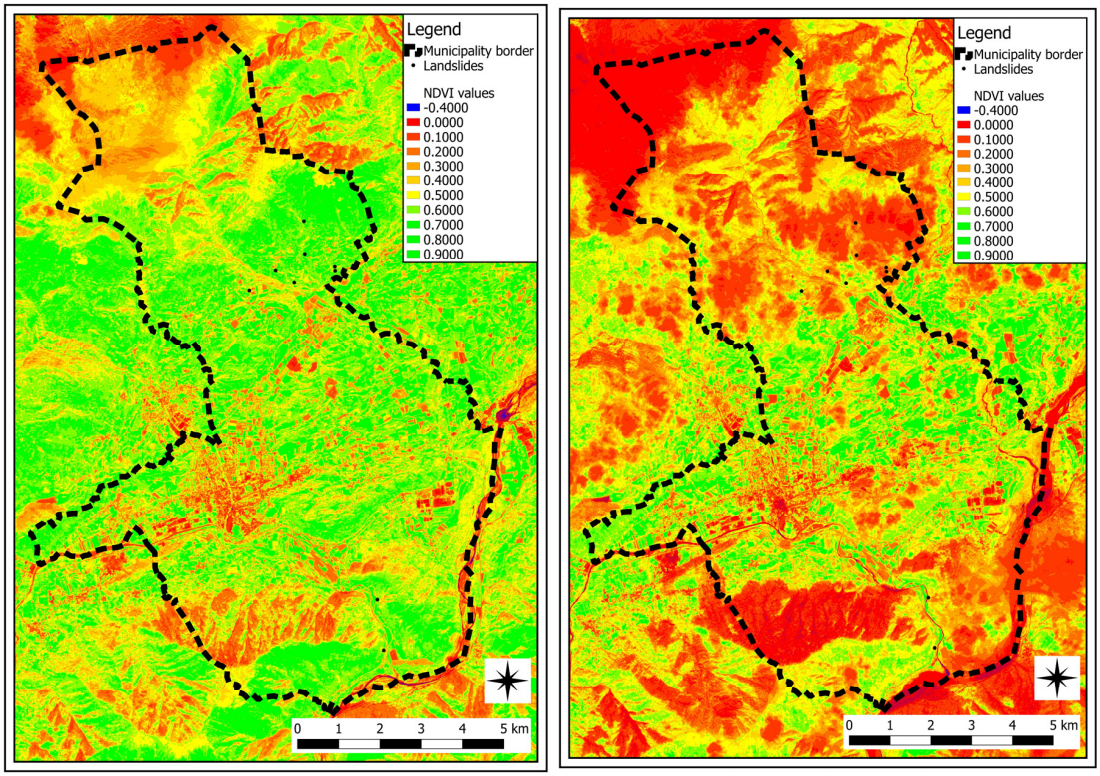

Figure 17. NDVI of the area before and after the event. Images from the satellite Sentinel-2B, acquisitions of 11 October 2018 (**a**) and 31 October 2018 (**b**).

As further proof of the influence of vegetation change even in the case of the nine landslides activated during the event, Table 2 is shown, which is certainly explanatory and shows a generalised decrease due to both vegetation felling and the decrease in cover resulting from landslide activation.

Table 2. The first column shows the landslide code, while the second column shows the average NDVI value in the landslide area before the event, and the third column shows the average NDVI value in the landslide area after the event.

Code Landslide	NDVI Before	NDVI After
025021_01c	0.70	0.50
025021_02c	0.60	0.40
025021_03c	0.70	0.20
025021_04c	0.60	0.20
025021_05c	0.60	0.20
025021_05c	0.60	0.20
025021_06c	0.60	0.50
025021_07c	0.60	0.30
025021_08c	0.40	0.30

Subsequently, based on the wind speed and direction values of the available weather stations, the area was modelled to assess the variation in speed determined by the topographic surface. To obtain this map, maximum wind gust data were taken from 2010 to 2022 (Figure 18).

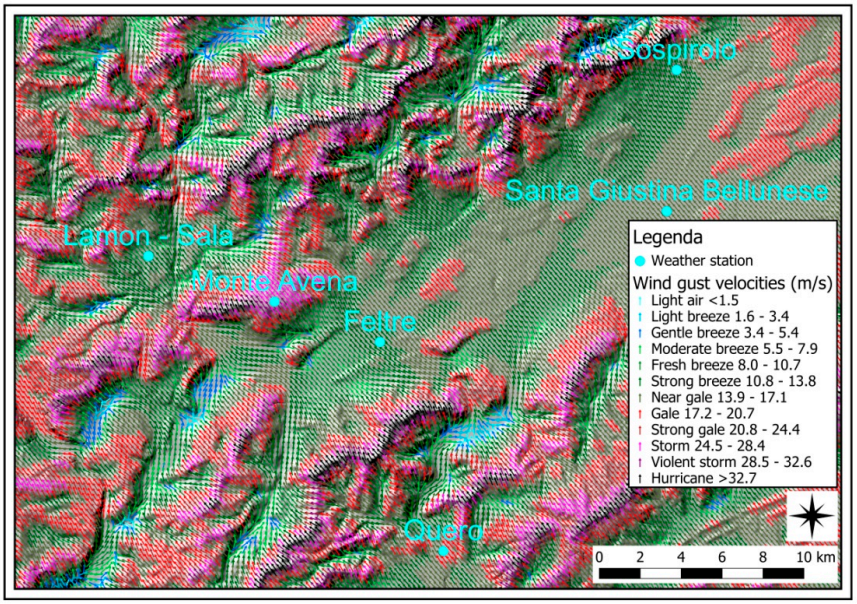

Figure 18. Wind gust modelling in the area.

The wind speed showed important differences from the weather stations, especially in the intensity of wind gusts. In particular, the ridges, some particularly steep slopes, and narrow valleys were noted to have produced significant accelerations characterised by black arrows marking hurricane category 1 speeds, i.e., greater than or equal to 32.7 m/s (Figure 18). On the basis of this map (Figure 18), wind speed and wind direction data from storm Vaia were taken and a map of susceptibility to tree felling by wind was developed, although it can be considered a map of susceptibility to wind damage in general. Then, a raster was made of the vector file of the maximum wind gust speed, which represents precisely the wind speed over the entire study area. The Beaufort scale was used to provide a classification, dividing the map into four values: the first at low susceptibility with winds up to 13.9 m/s, the second at medium-low susceptibility up to 20.8 m/s, the third at medium-high susceptibility up to 28.4 m/s, and the fourth at high susceptibility, above 28.4 m/s (Figure 19).

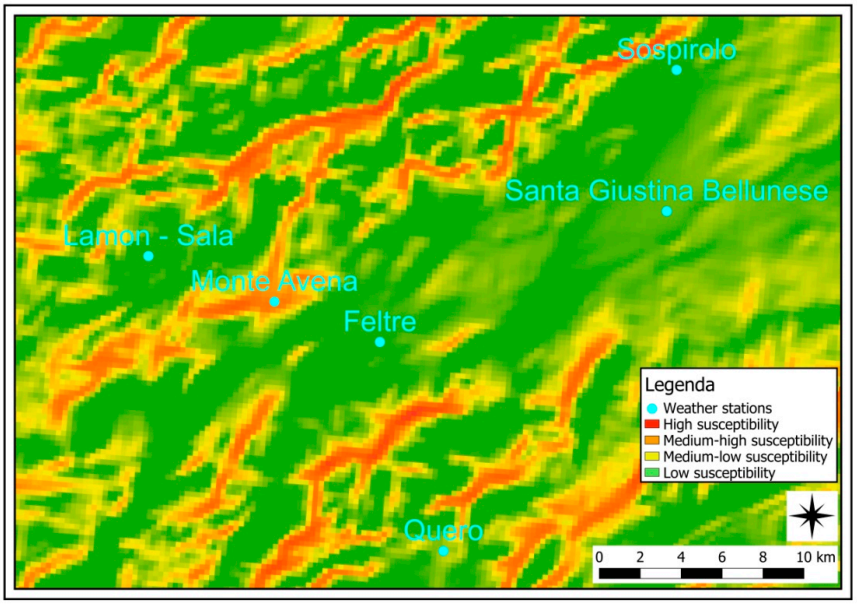

Figure 19. Wind damage susceptibility map.

The highest susceptibility values, characterised by the colour red, were spatially located in Figure 19. The Veneto Region's census of trees felled by wind, superimposed on the wind model (wind damage susceptibility map), shows a localisation of damage in areas with the highest increase in speed (Figure 20). There is a good correspondence between the highest wind speed values and the greatest damage, with a few extremely localised exceptions.

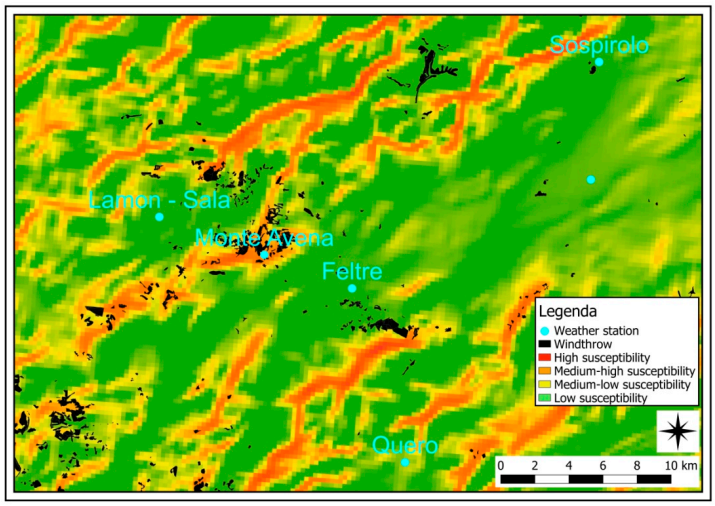

Figure 20. Susceptibility map with overlay of tree felling areas.

3.3. Susceptibility of the Municipality of Feltre to an Extreme Event

On the basis of the two susceptibility maps drawn up, i.e., the landslide map and the tree-felling map, a general susceptibility map was drawn up. This summary susceptibility map would express the fragility of a territory, in this case that of the municipality of Feltre, to an extreme event. By means of GIS software, the two maps were combined primarily by assessing only the degree of hazard to which a given territory may be subjected on a scale of 1 to 4 (Figure 21), always taking the highest susceptibility value between landslide susceptibility (Figure 6) and tree felling (Figure 9).

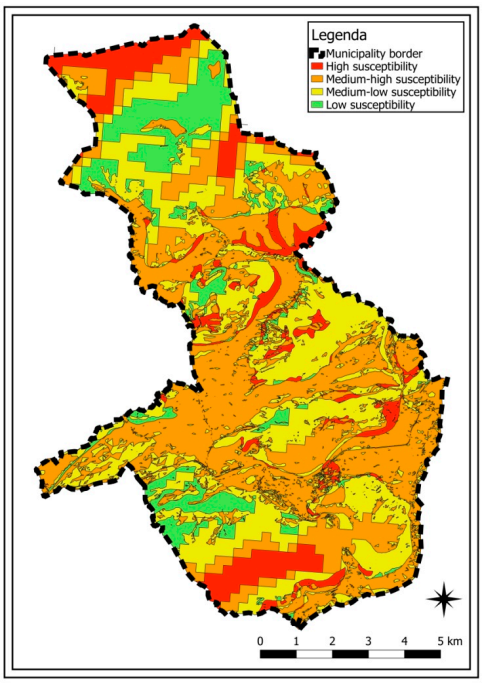

Figure 21. Combined extreme event susceptibility map obtained by averaging the two susceptibilities analysed.

Finally, a last map was drawn up that can be of immediate use to land planners, because it allows them to assess both geomorphological susceptibilities, i.e., from landslides, and biological susceptibility, i.e., from tree felling. To do this, all possible combinations of susceptibility were considered, as shown in the legend in Figure 22, to allow the two maps to be synthesised and to have a single tool to consult.

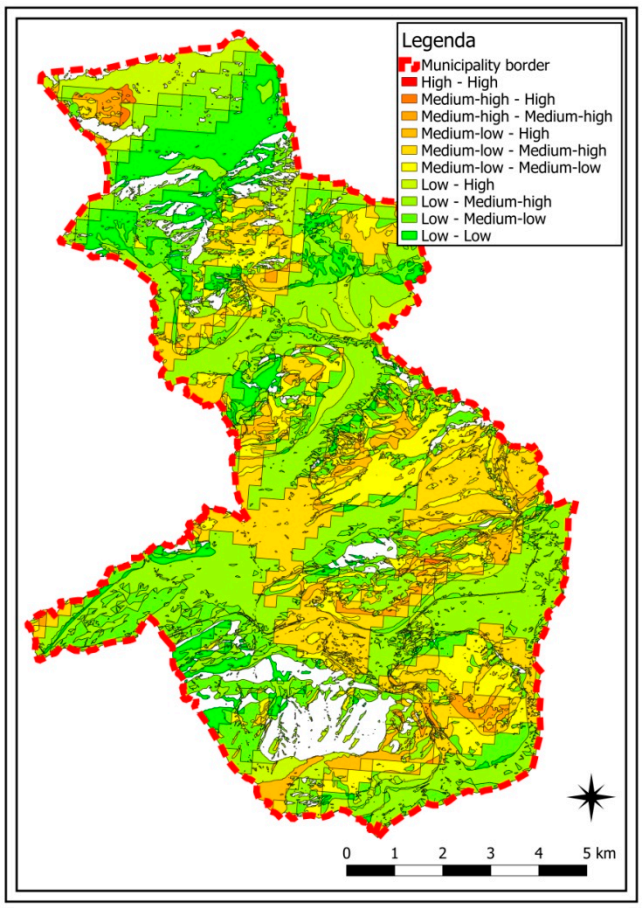

Figure 22. Extreme event susceptibility map combining susceptibility to wind damage and landslides.

4. Discussion

The assessment of susceptibility to landslides and tree felling in a given area is a highly innovative aspect of this study, as there are no other studies in the scientific literature that combine these two aspects by relating them to an extreme climatic event. Regarding the landslide susceptibility part of an extreme event, there are some examples in the literature that relate landslide susceptibility to extreme climatic events, finding a certain relationship [33,34]. Recent research has used binary logistic regression to predict the possible activation of landslides following an extreme event, hence a different landslide susceptibility map [35]. However, in many cases, the approaches to susceptibility maps are more classical and take numerous parameters into account, without taking into account extreme precipitation events [36]. At the same time, wind was evaluated by means of an analysis aimed at assessing modelling and thus its role in the felling and damage of plants, a topic already addressed in the past by other studies [37,38]. The strong winds in particular were extremely significant in this analysis, as the analysis of the weather stations did not indicate gust values of such a magnitude as to produce such damage to the environment, but after modelling, the topographical influence was highlighted, which led to the identification of areas in which the flow accelerated significantly. Analyses of tree felling in the literature have been conducted mainly in urban environments, assuming various wind magnitudes, in order to assess the damage to which the various species are subjected and which can also produce a non-negligible risk, precisely because they are

present in an urban environment [39]. The software used for wind modelling is much more frequently used in the literature for fire analysis and not as an extreme event damage analysis [40]. This study also carried out an important satellite analysis, assessing tree felling through the NDVI and comparing it through an additional census carried out in the municipality. Both of these were fully verified by the wind modelling, which showed a very good match with the calculated peak speeds. In fact, it was shown that the highest wind speeds were achieved predominantly in those areas where there had been the greatest felling of trees. In the literature, NDVI has also been used in some cases to assess the decline of individual forest species [41,42] or even how a change in climate is reflected on vegetation [43], and, in some cases, windthrown trees due to windstorms have been studied using the NDVI [44].

Finally, an attempt was made to give a geological/geomorphological explanation for the types of damage suffered by the trees, and it appears that there is a distinction between uprooted and broken trees based on the type of substrate present. Uprooted trees are mainly present where there is a substrate composed of deposits, moraine, and gravitational, which according to our hypothesis are less consolidated and mechanically poor, also due to the presence of minor processes in progress. The braked trees are instead localised where the substrate is characterised by bedrock and very little cover. The importance of the substrate for the stability of forest species is also demonstrated by numerous other research studies [45]. It would be important as a further research development not only to assess the influence of substrates more accurately, but also to distinguish by forest species and planting pattern. These results, which are corroborated in the existing scientific literature, make it possible to draw up an absolute rarity in the analysis of potential slope stability, namely the extreme event susceptibility map. Wind and precipitation are triggering factors that should be thoroughly investigated in the case of an extreme event, in order to provide a new tool for analysing the potential hazard of an area subjected to severe meteorological stress.

5. Conclusions

This study proposes a methodology to assess the susceptibility of a territory to an extreme event consisting of both heavy rainfall and strong winds. With regard to landslide susceptibility, a very conservative model was devised, assessing susceptibility on the basis of eight geomorphological–environmental parameters and comparing activated landslides with portions of land that are apparently stable but could be activated in the event of an extreme climatic event. For the wind damage susceptibility map, the modelling obtained was very interesting as it allowed an understanding of the abatements that was not comprehensible from an analysis of the values measured at certain weather stations alone due to insufficiently high values. The combined susceptibility map synthesises geological–geomorphological and environmental issues. The result is a tool that, appropriately calibrated, can be of great use to institutions involved in land management, allowing rapid decisions to be made. Furthermore, it could make it possible to assess a priori the resilience to an extreme event of a given area, in order to prepare the appropriate countermeasures and consequently save funds that would otherwise be needed to manage the emergency.

Author Contributions: Conceptualization, G.A., M.G. and G.P.; methodology, G.A. and M.G.; software, M.G.; validation, G.A. and D.A.; formal analysis, G.A.; investigation, G.A.; resources, M.G. and G.P.; data curation, G.A.; writing—original draft preparation, M.G.; writing—review and editing, D.A.; visualization, G.A.; supervision, G.P. and D.A.; project administration, G.P. All authors have read and agreed to the published version of the manuscript.

Funding: This research received no external funding.

Institutional Review Board Statement: Not applicable.

Informed Consent Statement: Not applicable.

Data Availability Statement: Not applicable.

Conflicts of Interest: The authors declare no conflict of interest.

References

1. Rahmstorf, S.; Coumou, D. Increase of extreme events in a warming world. *Proc. Natl. Acad. Sci. USA* **2011**, *108*, 17905–17909. [CrossRef] [PubMed]
2. Gentilucci, M.; Ghanem, M.; Barbieri, M. Statistical Analysis of Wind to Assess Climate Change (Central Italy). In *Conference of the Arabian Journal of Geosciences*; Springer: Berlin/Heidelberg, Germany, 2019; pp. 11–13.
3. Hwang, Y.T.; Frierson, D.M. Increasing atmospheric poleward energy transport with global warming. *Geophys. Res. Lett.* **2010**, *37*, L24807. [CrossRef]
4. Pithan, F.; Svensson, G.; Caballero, R.; Chechin, D.; Cronin, T.; Ekman, A.M.; Neggers, R.; Shupe, M.; Solomon, A.; Tjernstrom, M.; et al. Role of air-mass transformations in exchange between the Arctic and mid-latitudes. *Nat. Geosci.* **2018**, *11*, 805–812. [CrossRef]
5. Trinh, M.T.; Lee, G.; Oh, S.; Nguyen, T.H.V. Effect of extreme rainfall on cut slope stability: Case study in Yen Bai City, Viet Nam. *J. Korean GEO-Environ. Soc.* **2015**, *16*, 23–32.
6. Wong, J.L.; Lee, M.L.; Teo, F.Y.; Liew, K.W. A Review of Impacts of Climate Change on Slope Stability. In *Climate Change and Water Security. Lecture Notes in Civil Engineering*; Kolathayar, S., Mondal, A., Chian, S.C., Eds.; Springer: Singapore, 2022; Volume 178.
7. Zimmerman, J.K.; Everham III, E.M.; Waide, R.B.; Lodge, D.J.; Taylor, C.M.; Brokaw, N.V. Responses of tree species to hurricane winds in subtropical wet forest in Puerto Rico: Implications for tropical tree life histories. *J. Ecol.* **1994**, *82*, 911–922. [CrossRef]
8. Rossi, G.; Cancelliere, A. Managing drought risk in water supply systems in Europe: A review. *Int. J. Water Resour. Dev.* **2013**, *29*, 272–289. [CrossRef]
9. Rosenzweig, C.; Tubiello, F.N.; Goldberg, R.; Mills, E.; Bloomfield, J. Increased crop damage in the US from excess precipitation under climate change. *Glob. Environ. Chang.* **2002**, *12*, 197–202. [CrossRef]
10. Gentilucci, M.; Barbieri, M.; Burt, P. Climate and territorial suitability for the Vineyards developed using GIS techniques. In *Conference of the Arabian Journal of Geosciences*; Springer: Berlin/Heidelberg, Germany, 2018; pp. 11–13.
11. Gentilucci, M.; Moustafa, A.A.; Abdel-Gawad, F.K.; Mansour, S.R.; Coppola, M.R.; Caserta, L.; Inglese, S.; Pambianchi, G.; Guerriero, G. Advances in Egyptian mediterranean coast climate change monitoring. *Water* **2021**, *13*, 1870. [CrossRef]
12. Ayalew, L.; Yamagishi, H. The application of GIS-based logistic regression for landslide susceptibility mapping in the Kakuda-Yahiko Mountains, Central Japan. *Geomorphology* **2005**, *65*, 15–31. [CrossRef]
13. Wang, Y.; Fang, Z.; Hong, H. Comparison of convolutional neural networks for landslide susceptibility mapping in Yanshan County. *China. Sci. Total Environ.* **2019**, *666*, 975–993. [CrossRef]
14. Shit, P.K.; Bhunia, G.S.; Maiti, R. Potential landslide susceptibility mapping using weighted overlay model (WOM). *Model. Earth Syst. Environ.* **2016**, *2*, 21. [CrossRef]
15. Goyes-Peñafiel, P.; Hernandez-Rojas, A. Landslide susceptibility index based on the integration of logistic regression and weights of evidence: A case study in Popayan, Colombia. *Eng. Geol.* **2021**, *280*, 105958. [CrossRef]
16. Gentilucci, M.; Materazzi, M.; Pambianchi, G. Statistical Analysis of Landslide Susceptibility, Macerata Province (Central Italy). *Hydrology* **2021**, *8*, 5. [CrossRef]
17. Marjanović, M.; Kovačević, M.; Bajat, B.; Voženílek, V. Landslide susceptibility assessment using SVM machine learning algorithm. *Eng. Geol.* **2011**, *123*, 225–234. [CrossRef]
18. Gassner, C.; Promper, C.; Beguería, S.; Glade, T. Climate change impact for spatial landslide susceptibility. In *Engineering Geology for Society and Territory*; Springer: Berlin/Heidelberg, Germany, 2015; Volume 1, pp. 429–433.
19. Sabatakakis, N.; Koukis, G.; Vassiliades, E.; Lainas, S. Landslide susceptibility zonation in Greece. *Nat. Hazards* **2013**, *65*, 523–543. [CrossRef]
20. Lombardo, L.; Cama, M.; Maerker, M.; Rotigliano, E. A test of transferability for landslides susceptibility models under extreme climatic events: Application to the Messina 2009 disaster. *Nat. Hazards* **2014**, *74*, 1951–1989. [CrossRef]
21. Martin, T.J.; Ogden, J. Wind damage and response in New Zealand forests: A review. *N. Z. J. Ecol.* **2006**, *30*, 295–310.
22. Quine, C.P.; Gardiner, B.A.; Moore, J. Wind disturbance in forests: The process of wind created gaps, tree overturning, and stem breakage. In *Plant Disturbance Ecology*; Academic Press: Cambridge, MA, USA, 2021; pp. 117–184.
23. Peterson, C.J. Change in tree spatial pattern after severe wind disturbance in four North American northern hardwood and sub-boreal forests. *Front. For. Glob. Chang.* **2020**, *3*, 57. [CrossRef]
24. Zhou, B.; Wang, X.; Cao, Y.; Ge, X.; Gu, L.; Meng, J. Damage assessment to subtropical forests following the 2008 Chinese ice storm. *Iforest-Biogeosciences For.* **2017**, *10*, 406. [CrossRef]
25. Bonazountas, M.; Kallidromitou, D.; Kassomenos, P.A.; Passas, N. Forest fire risk analysis. *Hum. Ecol. Risk Assess.* **2005**, *11*, 617–626. [CrossRef]
26. Campisano, A.; Gnecco, I.; Modica, C.; Palla, A. Designing domestic rainwater harvesting systems under different climatic regimes in Italy. *Water Sci. Technol.* **2013**, *67*, 2511–2518. [CrossRef] [PubMed]
27. Offenthaler, I.; Felderer, A.; Formayer, H.; Glas, N.; Leidinger, D.; Leopold, P.; Schmidt, A.; Lexer, M.J. Threshold or Limit? Precipitation Dependency of Austrian Landslides, an Ongoing Challenge for Hazard Mapping under Climate Change. *Sustainability* **2020**, *12*, 6182. [CrossRef]

28. ARPAV (Agenzia Regionale per la Protezione dell'Ambiente Veneto). *Carta Della Natura del Veneto Alla Scala 1:50.000*; Rapporti No. 106/2010; ISPRA: Roma, Italy, 2010.
29. Costa, V.; Doglioni, C.; Grandesso, P.; Masetti, D.; Pellegrini, G.B.; Tracanella, E. Carta Geologica d'Italia alla scala 1:50.000. Note Illustrative del F°63 Belluno, 74; 1979. Available online: https://www.isprambiente.gov.it/Media/carg/note_illustrative/63_Belluno.pdf (accessed on 1 August 2022).
30. Tarquini, S.; Isola, I.; Favalli, M.; Battistini, A. TINITALY, A Digital Elevation Model of Italy with a 10 Meters Cell Size (Version 1.0) [Data Set]. Istituto Nazionale di Geofisica e Vulcanologia (INGV). 2007. Available online: https://data.ingv.it/dataset/185#additional-metadata (accessed on 1 August 2022).
31. Ehsan, S.; Kazem, D. Analysis of land use-land covers changes using normalized difference vegetation index (NDVI) differencing and classification methods. *Afr. J. Agric. Res.* **2013**, *8*, 4614–4622. [CrossRef]
32. Forthofer, J.M.; Butler, B.W.; Wagenbrenner, N.S. A comparison of three approaches for simulating fine-scale surface winds in support of wildland fire management. Part I. Model formulation and comparison against measurements. *Int. J. Wildland Fire.* **2014**, *23*, 969–981. [CrossRef]
33. Phien-Wej, N.; Nutalaya, P.; Aung, Z.; Zhibin, T. Catastrophic landslides and debris flows in Thailand. *Bull. Int. Assoc. Eng. Geol.-Bull. De L'assoc. Int. De Géologie De L'ingénieur* **1993**, *48*, 93–100. [CrossRef]
34. Chen, X.; Chen, W. GIS-based landslide susceptibility assessment using optimized hybrid machine learning methods. *Catena* **2021**, *196*, 104833. [CrossRef]
35. Jones, J.N.; Boulton, S.J.; Bennett, G.L.; Stokes, M.; Whitworth, M.R. Temporal variations in landslide distributions following extreme events: Implications for landslide susceptibility modeling. *J. Geophys. Res. Earth Surf.* **2021**, *126*, e2021JF006067. [CrossRef]
36. Guri, P.K.; Patel, R.C. Spatial prediction of landslide susceptibility in parts of Garhwal Himalaya, India, using the weight of evidence modelling. *Environ. Monit. Assess.* **2015**, *187*, 1–25. [CrossRef] [PubMed]
37. Baker, W.L.; Flaherty, P.H.; Lindemann, J.D.; Veblen, T.T.; Eisenhart, K.S.; Kulakowski, D.W. Effect of vegetation on the impact of a severe blowdown in the southern Rocky Mountains, USA. *For. Ecol. Manag.* **2002**, *168*, 63–75. [CrossRef]
38. Zielonka, T.; Holeksa, J.; Fleischer, P.; Kapusta, P. A tree-ring reconstruction of wind disturbances in a forest of the Slovakian Tatra Mountains, Western Carpathians. *J. Veg. Sci.* **2010**, *21*, 31–42. [CrossRef]
39. Foran, C.M.; Baker, K.M.; Narcisi, M.J.; Linkov, I. Susceptibility assessment of urban tree species in Cambridge, MA, from future climatic extremes. *Environ. Syst. Decis.* **2015**, *35*, 389–400. [CrossRef]
40. Sanjuan, G.; Brun, C.; Margalef, T.; Cortés, A. Wind field uncertainty in forest fire propagation prediction. *Proc. Comput. Sci.* **2014**, *29*, 1535–1545. [CrossRef]
41. Navarro, A.; Catalao, J.; Calvao, J. Assessing the use of Sentinel-2 time series data for monitoring Cork Oak decline in Portugal. *Remote Sens.* **2019**, *11*, 2515. [CrossRef]
42. Fiore, N.M.; Goulden, M.L.; Czimczik, C.I.; Pedron, S.A.; Tayo, M.A. Do recent NDVI trends demonstrate boreal forest decline in Alaska? *Environ. Res. Lett.* **2020**, *15*, 095007. [CrossRef]
43. Gentilucci, M.; Barbieri, M.; Materazzi, M.; Pambianchi, G. Effects of Climate Change on Vegetation in the Province of Macerata (Central Italy). In *Advanced Studies in Efficient Environmental Design and City Planning*; Springer: Berlin/Heidelberg, Germany, 2021; pp. 463–474.
44. Camarero, J.J.; Colangelo, M.; Gazol, A.; Pizarro, M.; Valeriano, C.; Igual, J.M. Effects of windthrows on forest cover, tree growth and soil characteristics in drought-prone pine plantations. *Forests* **2021**, *12*, 817. [CrossRef]
45. Lewis, M.E. Windfall disturbance in a piedmont uplands forest. *Southeast. Geogr.* **1991**, *31*, 1–14. [CrossRef]